

Air Force Institute of Technology

AFIT Scholar

Faculty Publications

6-2014

Copper Doping of ZnO Crystals by Transmutation of ^{64}Zn to ^{65}Cu : An Electron Paramagnetic Resonance and Gamma Spectroscopy Study

Matthew C. Recker

John W. McClory

Air Force Institute of Technology

Maurio S. Holston

Eric M. Golden

Nancy C. Giles

Air Force Institute of Technology

See next page for additional authors

Follow this and additional works at: <https://scholar.afit.edu/facpub>



Part of the [Atomic, Molecular and Optical Physics Commons](#), and the [Semiconductor and Optical Materials Commons](#)

Recommended Citation

Recker, M. C., McClory, J. W., Holston, M. S., Golden, E. M., Giles, N. C., & Halliburton, L. E. (2014). Copper doping of ZnO crystals by transmutation of ^{64}Zn to ^{65}Cu : An electron paramagnetic resonance and gamma spectroscopy study. *Journal of Applied Physics*, 115(24), 243706. <https://doi.org/10.1063/1.4885439>

This Article is brought to you for free and open access by AFIT Scholar. It has been accepted for inclusion in Faculty Publications by an authorized administrator of AFIT Scholar. For more information, please contact richard.mansfield@afit.edu.

Authors

Matthew C. Recker, John W. McClory, Maurio S. Holston, Eric M. Golden, Nancy C. Giles, and Larry E. Halliburton

Copper doping of ZnO crystals by transmutation of ^{64}Zn to ^{65}Cu : An electron paramagnetic resonance and gamma spectroscopy study

Cite as: J. Appl. Phys. **115**, 243706 (2014); <https://doi.org/10.1063/1.4885439>

Submitted: 03 June 2014 . Accepted: 14 June 2014 . Published Online: 26 June 2014

M. C. Recker, J. W. McClory, M. S. Holston, E. M. Golden, N. C. Giles, and L. E. Halliburton



View Online



Export Citation



CrossMark

ARTICLES YOU MAY BE INTERESTED IN

[A comprehensive review of ZnO materials and devices](#)

Journal of Applied Physics **98**, 041301 (2005); <https://doi.org/10.1063/1.1992666>

[Cu-doping of ZnO by nuclear transmutation](#)

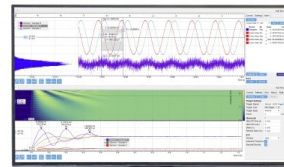
Applied Physics Letters **99**, 202109 (2011); <https://doi.org/10.1063/1.3662014>

[Identification of the zinc-oxygen divacancy in ZnO crystals](#)

Journal of Applied Physics **119**, 145701 (2016); <https://doi.org/10.1063/1.4945703>

Challenge us.

What are your needs for periodic signal detection?



Zurich
Instruments

Copper doping of ZnO crystals by transmutation of ^{64}Zn to ^{65}Cu : An electron paramagnetic resonance and gamma spectroscopy study

M. C. Recker,¹ J. W. McClory,^{1,a)} M. S. Holston,¹ E. M. Golden,¹ N. C. Giles,¹
and L. E. Halliburton²

¹*Department of Engineering Physics, Air Force Institute of Technology, Wright-Patterson Air Force Base, Ohio 45433, USA*

²*Department of Physics and Astronomy, West Virginia University, Morgantown, West Virginia 26506, USA*

(Received 3 June 2014; accepted 14 June 2014; published online 26 June 2014)

Transmutation of ^{64}Zn to ^{65}Cu has been observed in a ZnO crystal irradiated with neutrons. The crystal was characterized with electron paramagnetic resonance (EPR) before and after the irradiation and with gamma spectroscopy after the irradiation. Major features in the gamma spectrum of the neutron-irradiated crystal included the primary 1115.5 keV gamma ray from the ^{65}Zn decay and the positron annihilation peak at 511 keV. Their presence confirmed the successful transmutation of ^{64}Zn nuclei to ^{65}Cu . Additional direct evidence for transmutation was obtained from the EPR of Cu^{2+} ions (where ^{63}Cu and ^{65}Cu hyperfine lines are easily resolved). A spectrum from isolated Cu^{2+} ($3d^9$) ions acquired after the neutron irradiation showed only hyperfine lines from ^{65}Cu nuclei. The absence of ^{63}Cu lines in this Cu^{2+} spectrum left no doubt that the observed ^{65}Cu signals were due to transmuted ^{65}Cu nuclei created as a result of the neutron irradiation. Small concentrations of copper, in the form of $\text{Cu}^+\text{-H}$ complexes, were inadvertently present in our as-grown ZnO crystal. These $\text{Cu}^+\text{-H}$ complexes are not affected by the neutron irradiation, but they dissociate when a crystal is heated to 900 °C. This behavior allowed EPR to distinguish between the copper initially in the crystal and the copper subsequently produced by the neutron irradiation. In addition to transmutation, a second major effect of the neutron irradiation was the formation of zinc and oxygen vacancies by displacement. These vacancies were observed with EPR. © 2014 AIP Publishing LLC. [<http://dx.doi.org/10.1063/1.4885439>]

I. INTRODUCTION

Copper has been widely studied in ZnO for many years.^{1–11} These ions are often present at low concentrations ($< 5 \times 10^{16} \text{cm}^{-3}$) as a residual impurity in ZnO bulk crystals, thin films, and nanoparticles. Much higher concentrations can be achieved by doping during growth or by post-growth diffusion. Nuclear transmutation is an alternative method of doping ZnO with copper.^{12–17} Here, conversion of ^{64}Zn to ^{65}Cu allows uniform copper doping at precisely controlled levels. Isolated copper ions on zinc sites are acceptors, but they are generally believed to be very deep (several reports^{18,19} have placed the 0/– acceptor level approximately 160–190 meV below the conduction band). It may be possible for copper to form a complex with a nearby acceptor (e.g., a second substitutional copper or a zinc vacancy) or with a nearby donor and acceptor (i.e., an acceptor-donor-acceptor (ADA) complex) and thus create a shallow acceptor state that will contribute to *p*-type behavior in ZnO.^{20–22} Also, when present at high doping levels, copper ions may lead to ferromagnetic behavior at room temperature and make Cu-doped ZnO suitable for spintronic applications.^{23–26} Controlled doping with copper (as in the transmutation process) could, therefore, be important in developing proof-of-concept prototypes of practical ZnO-based devices.

Copper in ZnO can be present as Cu^+ ($3d^{10}$) or Cu^{2+} ($3d^9$) ions substituting for Zn^{2+} ions. As is customary, ionic notation is used to describe the different charge states of copper ions. A substitutional Cu^{2+} ion is a neutral acceptor (A^0) and a Cu^+ ion is a singly ionized acceptor (A^-). There is no reliable experimental evidence suggesting that copper occurs as an isolated interstitial in ZnO. Electron paramagnetic resonance (EPR) and near-infrared (NIR) absorption techniques are two direct high-resolution spectroscopy methods to monitor Cu^{2+} ions in ZnO crystals (i.e., the incomplete *d* shell of these ions gives rise to unique spectroscopic signatures).^{1–4,7–11} The Cu^{2+} EPR spectrum, with $g_{\parallel} = 0.729$ and $g_{\perp} = 1.520$, shows well-resolved hyperfine lines from ^{63}Cu and ^{65}Cu nuclei. Because of severe broadening at higher temperature due to a short spin-lattice relaxation time, this EPR spectrum can only be observed at temperatures below 9 K. Two NIR absorption bands at 5782 and 5820 cm^{-1} are internal transitions of the Cu^{2+} ions and also are best seen at low temperature. The Cu^+ ions have a filled *d* shell and are more difficult to monitor at low concentrations with optical or magnetic resonance techniques. An infrared vibrational band, observed at 3192 cm^{-1} at 10 K, provides a direct method to detect Cu^+ ions that have an adjacent hydrogen.^{5–7,9} This $\text{Cu}^+\text{-OH}^-$ absorption band broadens and shifts at higher temperature.

In the present paper, we use EPR and gamma spectroscopy to detect the transmutation of ^{64}Zn to ^{65}Cu in a single crystal of ZnO. The crystal was irradiated for 20 h in a

^{a)}Author to whom correspondence should be addressed. Electronic mail: John.McClory@afit.edu

nuclear reactor. The ^{64}Zn nuclei absorb thermal neutrons and form unstable ^{65}Zn nuclei that then convert to ^{65}Cu . The half-life of ^{65}Zn is 244 days. There is a 50.23% probability that a ^{65}Zn nucleus decays to an excited state of ^{65}Cu by electron capture and then emits a 1115.5 keV characteristic γ ray, there is a 48.35% probability that a ^{65}Zn nucleus decays directly to the ground state of ^{65}Cu by electron capture, and there is a 1.42% probability that the ^{65}Zn nucleus decays directly to the ground state of ^{65}Cu by positron emission (two 511 keV γ rays are produced when the positron is annihilated). Our gamma spectrum shows the emission of 1115.5 and 511 keV γ rays. With low-temperature EPR, we observe substitutional Cu^{2+} ions in our crystal. Fortunately, relative concentrations of ^{63}Cu and ^{65}Cu nuclei can be determined from the well-resolved hyperfine pattern associated with the Cu^{2+} EPR spectrum. By monitoring these EPR hyperfine lines, we show that a significant amount of ^{65}Cu was produced by nuclear transmutation. Since copper impurities are ubiquitous in nearly all ZnO, we caution that an investigation of the transmutation of ^{64}Zn to ^{65}Cu should account for any copper that is present before neutron irradiation. In our study, a comparison of the individual strengths of the ^{63}Cu and ^{65}Cu hyperfine lines in the Cu^{2+} EPR spectra allowed us to distinguish between the copper that was present before the neutron irradiation and the copper that was produced as a result of the neutron irradiation.

II. EXPERIMENTAL

Material from a bulk single crystal of ZnO grown by the seeded-vapor-transport method at Eagle-Picher (Miami, Oklahoma) was used in the present investigation. Two adjacent samples, each with approximate dimensions of $2.5 \times 4.0 \times 0.5 \text{ mm}^3$, were cut from a larger $10 \times 10 \times 0.5 \text{ mm}^3$ *c* plate supplied by the company. One sample was not neutron irradiated and instead was used to verify the presence of residual copper in the as-grown material. The other sample was irradiated with neutrons at the Ohio State University Nuclear Reactor Laboratory (Columbus, Ohio). This is a pool-type reactor operating at a maximum power of 450 kW. The ZnO sample was held in the central irradiation facility of the reactor for 20 h. The total neutron flux was $\sim 2.1 \times 10^{13} \text{ neutrons cm}^{-2}\text{s}^{-1}$ and the thermal neutron flux was $\sim 1.3 \times 10^{13} \text{ cm}^{-2}\text{s}^{-1}$. The temperature of the sample was not measured during the neutron irradiation, but the survival of zinc vacancies produced by the high-energy neutrons (see Sec. V) suggests that it was less than 150 °C. The activity of our sample 11 days after the irradiation was $89.2 \pm 0.4 \mu\text{Ci}$. In addition to the vapor-transport-grown crystal, we neutron irradiated a hydrothermally grown ZnO crystal (from Tokyo Denpa) to verify that the crystal growth method did not affect the transmutation of ^{64}Zn to ^{65}Cu .

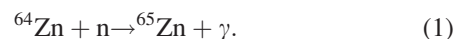
A Canberra high-purity germanium (HPGe) detector cooled with liquid nitrogen and a multi-channel analyzer were used to obtain the energy spectrum of the emitted gamma rays. The gamma spectrometer, located at the reactor facility, was calibrated using a multi-nuclide source from Amersham. A Bruker EMX spectrometer operating at 9.397 GHz was used to take the EPR data at the Air Force

Institute of Technology. The temperature was controlled with a helium-gas-flow system from Oxford Instruments. A helium-cadmium laser was used to illuminate samples at low temperature in the EPR cavity (approximately 15 mW of 442 nm light was incident on the sample). Estimates of the concentrations of defects contributing to the EPR spectra were obtained by making comparisons to a standard pitch sample provided by Bruker.

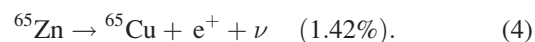
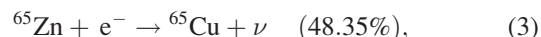
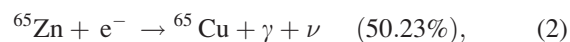
III. Zn ISOTOPES AND NEUTRON ABSORPTION

The five stable isotopes of zinc and their natural abundances²⁷ are ^{64}Zn (48.268%), ^{66}Zn (27.975%), ^{67}Zn (4.102%), ^{68}Zn (19.024%), and ^{70}Zn (0.631%). Two of these isotopes, ^{66}Zn and ^{67}Zn , are not of interest to the present study because they form a heavier, but stable, Zn isotope after absorbing a neutron. Also, absorption of neutrons by oxygen isotopes is not central to our study. Unstable ^{19}O is formed during the neutron irradiation, and decays to ^{19}F by beta emission. These ^{19}O nuclei have a short half-life (~ 26 s) and are not seen in gamma spectra taken days after the neutron irradiation. Fluorine at an oxygen site will be a donor in ZnO. As is the case for the other shallow donors in this material (e.g., Al and Ga), neutral fluorine donors when present are expected to have a “generic” effective-mass EPR signal near $g = 1.96$ with unresolved hyperfine.

Absorption of a neutron by ^{64}Zn leads to the creation of ^{65}Zn and the immediate release of a γ ray. The energy-dependent cross sections for this neutron-absorption reaction are known²⁸



The newly formed isotope, ^{65}Zn , is unstable with a half-life of 244 days and decays by one of the following three paths to ^{65}Cu . The relative probability for each decay path is indicated^{29–31}



These decay paths are illustrated in Fig. 1. Equations (2) and (3) represent electron capture paths where the ^{65}Zn nucleus captures an inner orbital electron to convert an excess proton to a neutron, thereby reducing the *Z* number of the nucleus and transmuting the nucleus to ^{65}Cu . A neutrino is always emitted in these decays. The first of the electron-capture paths occurs 50.23% of the time and results in an excited state of ^{65}Cu that then decays to its ground state with the emission of a 1115.5 keV characteristic γ ray. We use this γ -ray to verify that ^{65}Zn is produced in our samples. There is a small probability (0.0025%), and thus not important to the present study, for the excited state of ^{65}Cu to decay to an intermediate level and then to the ground state by emission of 344 and 770 keV γ rays. The second electron capture path, described by Eq. (3), goes directly to the ground state with no γ -ray emission. The decay path in Eq. (4) is by β^+ directly to the ground state. This conversion of a proton to a neutron

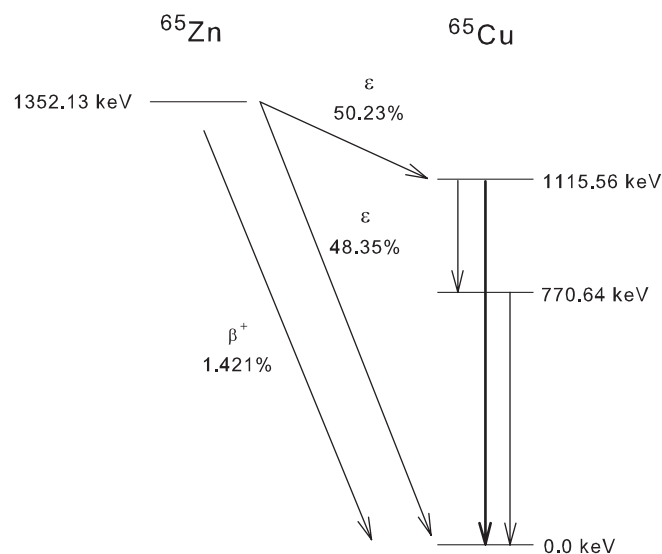


FIG. 1. The ^{65}Zn to ^{65}Cu nuclear decay scheme. Two of the paths (50.23% and 48.35%) are by electron capture (ϵ) and one path (1.421%) is by positron emission (β^+).

is accompanied by the emission of a positron and a neutrino. Two 511 keV γ rays are then produced when the positron annihilates with an electron.

Absorption of a neutron by ^{68}Zn produces unstable ^{69}Zn or $^{69\text{m}}\text{Zn}$ nuclei which then decay to ^{69}Ga .³² The half-life of ^{69}Zn is 56 min and the half-life of $^{69\text{m}}\text{Zn}$ is 13.76 h. Similarly, absorption of a neutron by ^{70}Zn produces unstable ^{71}Zn or $^{71\text{m}}\text{Zn}$ nuclei which then decay to ^{71}Ga .³² The half-life of ^{71}Zn is 2.4 min and the half-life of $^{71\text{m}}\text{Zn}$ is 3.97 h. Because of these relatively short half-lives, emitted γ rays in the decay schemes are not usually observed when gamma spectra are taken more than a few days after a neutron irradiation. The Ga^{3+} ($3d^{10}$) ions that are formed from the Zn^{2+} ($3d^{10}$) ions as a result of the absorption of neutrons by ^{68}Zn and ^{70}Zn are already singly ionized shallow donors. When the Fermi level is high or when the crystal is illuminated at low temperature with near-band-edge light, these singly ionized donors convert to their neutral charge state and contribute to the effective-mass EPR signal near $g = 1.96$. Since individual hyperfine lines from the ^{69}Ga and ^{71}Ga nuclei are not resolved in this shallow-donor spectrum,³³ the EPR technique does not readily distinguish between the Ga ions that are produced by transmutation and the Ga ions that are introduced during crystal growth.

IV. RESULTS FROM GAMMA SPECTROSCOPY

The gamma spectrum of our neutron-irradiated ZnO crystal, recorded approximately 10 days after the irradiation, is shown in Fig. 2. It is presented as a semi-log plot to clearly illustrate that the less-intense features (i.e., the Compton edge at 907.6 keV, the Compton continuum, and the backscatter peak at 223 keV) are in the proper positions for ^{65}Zn . The dominant features in the gamma spectrum are the peaks near 511 and 1115.5 keV.

The gamma spectrometer placed the lower-energy γ -ray peak at 510.728 keV, which is close to but not exactly 511 keV. There is another nucleus that emits a γ ray at this

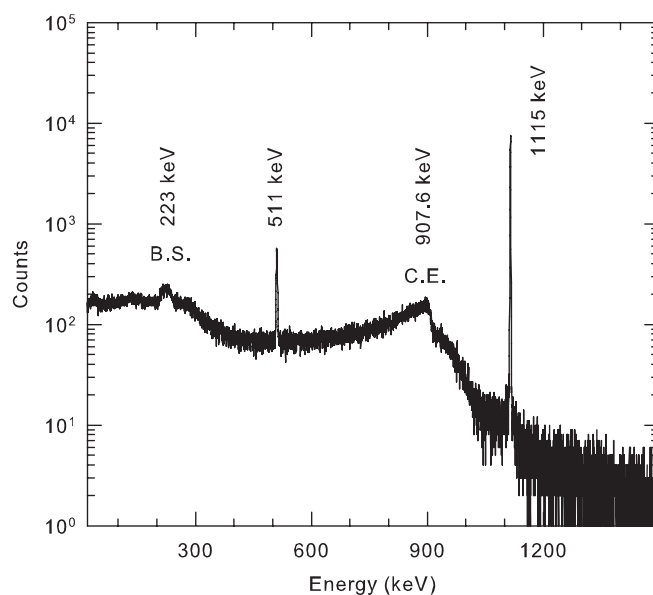


FIG. 2. Gamma spectrum of ZnO taken 10 days after a neutron irradiation. The Compton edge (C.E.) and backscatter (B.S.) peaks are clearly visible in this semi-log plot and are located at the expected positions for ^{65}Zn .

energy (^{208}Tl at 510.77 keV),³⁴ but it is not responsible for the peak at 511 keV in Fig. 2 because a short half-life (3.053 min) means that it would have decayed below the detection limit of the spectrometer long before the spectrum in Fig. 2 was recorded. Thus, the peak near 511 keV in Fig. 2 must be an annihilation peak, as expected for ^{65}Zn . We attribute the slight offset in measured energy to small systematic errors in the energy calibration of the gamma spectrometer. The observation of a 511 keV peak alone, however, does not establish the presence of ^{65}Zn in a neutron-irradiated sample because many isotopes decay by positron emission.

Our gamma spectrometer placed the most intense γ -ray peak in Fig. 2 at 1114.98 keV. This is close to the expected value of 1115.5 keV for ^{65}Zn , but there are two other possibilities. These are ^{127}Sn (1114.3 keV) and ^{65}Ni (1115.5 keV). These isotopes can be readily dismissed, however, because their short half-lives (2.1 and 2.5 h, respectively) mean that they would have decayed away long before our spectrum in Fig. 2 was recorded. To verify that the 1115 keV peak is due to ^{65}Zn , the relative intensities of the peaks at 511 and 1115 keV in Fig. 2 are compared. If they are due to ^{65}Zn , then 50.23% of the decays will result in a 1115 keV γ ray and 1.42% will result in a positron which creates two 511 keV photons when it annihilates. Thus, the predicted ratio of counts from our detector³⁵ for the two peaks should be 1.42 to 25.115, or simply 0.0565. After taking into account the energy-dependent absolute efficiency of the detector at the energies where γ rays are being monitored, we find that the experimental ratio of counts for the two peaks is 0.0559, which closely matches the predicted value. This establishes that the peaks at 511 and 1115 keV in Fig. 2 are due to the long-half-life decay of ^{65}Zn .

V. RESULTS FROM ELECTRON PARAMAGNETIC RESONANCE

The ZnO crystals used in this investigation contained small amounts of copper introduced during growth. In our

as-grown crystals, this copper is present as Cu^+ ($3d^{10}$) ions on a Zn^{2+} site, with no unpaired spins and thus no EPR signal. These Cu^+ acceptor ions are charge-compensated (i.e., passivated) by an adjacent OH^- ion at an oxygen site.³⁶ The hydrogen can be “driven” from the Cu^+ ions by heating a crystal in air to 900°C . This leaves isolated substitutional Cu^+ ions that can then be converted to Cu^{2+} ions with near-band-edge laser light when the temperature is below approximately 6 K.⁸ The resulting substitutional Cu^{2+} ions have a characteristic EPR spectrum that is easily monitored at temperatures near 6 K.^{1,3,4} This production of Cu^{2+} ions by removing the hydrogen at high temperature has been observed by Lavrov *et al.*⁹ in near-infrared-absorption experiments on hydrothermally grown ZnO crystals and has been computationally modeled by Hu and Pan.³⁷ A similar thermally induced dissociation behavior has been reported for nitrogen-hydrogen (N-H) complexes in ZnO crystals.^{33,38,39}

The Cu^{2+} EPR spectrum in Fig. 3(a) verifies that copper was present in our as-grown ZnO crystals. One of the two similar crystals cut from the original c plate was held at 900°C in air for 1 h (the other crystal was neutron irradiated without being heated to 900°C). This heat treatment of the unirradiated crystal produced the EPR spectrum from substitutional Cu^{2+} ($3d^9$) ions shown in Fig. 3(a). These data were taken at 6 K with the magnetic field perpendicular to the c axis (at an arbitrary direction in the basal plane) and with 442 nm laser light on the crystal. There were no Cu^{2+} EPR lines in the 380–500 mT field region in this as-grown crystal before heating to 900°C as the copper was then all present

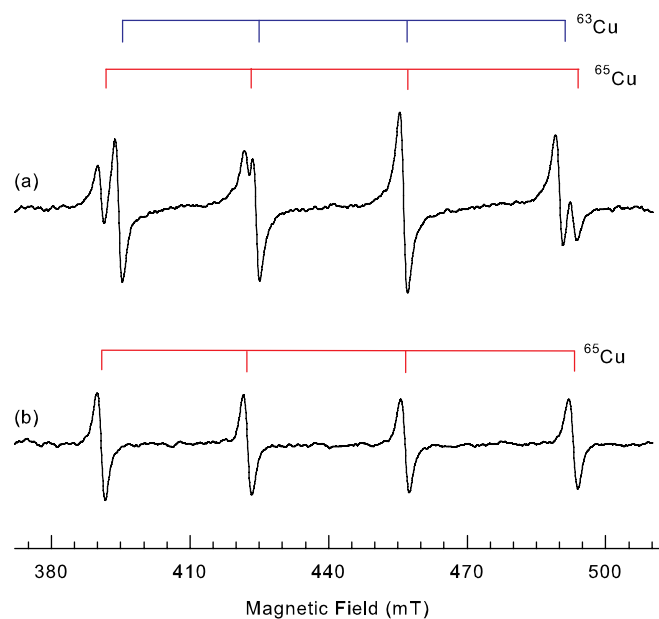


FIG. 3. EPR spectra of Cu^{2+} ions in ZnO illustrating (a) ^{63}Cu and ^{65}Cu present in the as-grown crystal and (b) ^{65}Cu produced by transmutation in the neutron-irradiated crystal. These data were obtained at 6 K with the magnetic field perpendicular to the c axis. The sample used for trace (a) was annealed for 1 h in air at 900°C , but was not neutron irradiated. The sample used for trace (b) was neutron irradiated approximately 180 days before taking the EPR spectrum. This latter sample was not annealed at 900°C before the neutron irradiation.

as Cu^+ ($3d^{10}$) ions with an adjacent hydrogen. Heating the unirradiated crystal to 900°C removed the hydrogen and left isolated Cu^+ ions. The Fermi level is high in this vapor-transport-grown crystal, and laser light was needed in Fig. 3(a) to convert the Cu^+ ions to Cu^{2+} ions at low temperature (by “moving” electrons to singly ionized donors).

A stick diagram above the Cu^{2+} EPR spectrum in Fig. 3(a) identifies the individual lines from ^{63}Cu and ^{65}Cu .^{1,3,4,8} Both isotopes have a nuclear spin $I=3/2$ and they produce similar hyperfine patterns consisting of four equally intense and equally spaced lines (the number of hyperfine lines from an isotope is equal to $2I+1$). The lines from ^{63}Cu nuclei have a slightly smaller separation than the lines from ^{65}Cu nuclei. This reflects the different nuclear magnetic moments of the two Cu isotopes ($^{63}\mu=+2.2273\beta_n$ and $^{65}\mu=+2.3816\beta_n$, where β_n is the nuclear magneton).⁴⁰ Also, the ^{63}Cu hyperfine lines are more intense than the ^{65}Cu hyperfine lines because the natural abundances of ^{63}Cu and ^{65}Cu are 69.15% and 30.85%, respectively.²⁷ As seen in Fig. 3(a), the inner two lines from each isotope nearly coincide, but the outer lines from the two isotopes are easily distinguished.

The EPR spectrum from our neutron-irradiated ZnO crystal is shown in Fig. 3(b). This spectrum was taken approximately 180 days after the 20 h neutron irradiation. The measurement temperature was 6 K and the magnetic field was perpendicular to the c axis. In Fig. 3(b), 442 nm laser light was not on the sample. The only hyperfine lines in this Cu^{2+} EPR spectrum are from the ^{65}Cu nuclei created by the slow decay of ^{65}Zn following the neutron irradiation. The ^{63}Cu and ^{65}Cu nuclei incorporated in the crystal during growth are all present as nonparamagnetic Cu^+ ions with adjacent hydrogens and thus are not contributing to the spectrum in Fig. 3(b). These neutral $\text{Cu}^+\text{-H}$ complexes have not dissociated at this stage because the temperature of the crystal did not exceed $\sim 150^\circ\text{C}$ during the neutron irradiation. The concentration of transmuted Cu^{2+} ions in the spectrum in Fig. 3(b) is estimated to be approximately $3.7 \times 10^{16} \text{cm}^{-3}$. Although not shown, a Cu^{2+} EPR spectrum very similar to that in Fig. 3(b) was obtained without laser light from our hydrothermally grown ZnO crystal 180 days after it was neutron irradiated for 20 h. This spectrum contained only ^{65}Cu hyperfine lines since the hydrothermal crystal had not been thermally annealed at 900°C . As expected, the concentrations of transmuted Cu^{2+} ions were similar in the crystals grown by different methods (i.e., seeded-vapor-transport vs. hydrothermal). To ensure a valid comparison, the two crystals received the same neutron dose and had the same delay time (i.e., 180 days) before the EPR measurements.

In addition to the transmutation of ^{64}Zn to ^{65}Cu , the neutron irradiation produced zinc and oxygen vacancies by a momentum-conserving displacement process initiated by the high-energy neutrons. Figure 4 shows an EPR spectrum obtained at 30 K with low microwave power ($3.2 \mu\text{W}$). The magnetic field was along the c axis and 442 nm laser light was on the sample. The line at 336.60 mT has been assigned to singly ionized oxygen vacancies⁴¹ (V_O^+) and the lines at 333.05 and 335.06 mT have been assigned to singly ionized nonaxial and axial zinc vacancies (V_{Zn}^-), respectively.^{42,43}

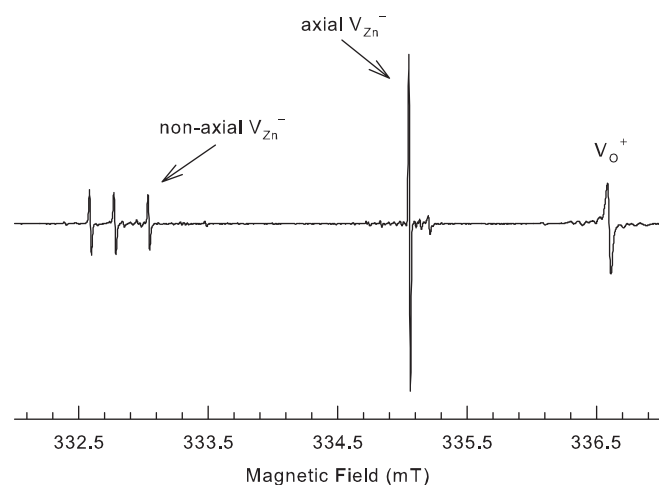


FIG. 4. EPR spectrum showing the singly ionized zinc and oxygen vacancy signals produced by the neutron irradiation. These data were obtained at 30 K. The microwave power was low ($3.2 \mu\text{W}$), the magnetic field was parallel to the c axis, and the sample was exposed to 442 nm laser light while the spectrum was recorded.

The two additional lines at 332.59 and 332.78 mT have been previously reported, but not identified.⁴⁴ Because their positions are near the nonaxial zinc vacancy line at 333.05 mT, we suggest that these lines may be from nonaxial singly ionized zinc vacancies that have a nearby perturbing impurity. Candidates for the perturbing entities are Ga^{3+} and Al^{3+} ions on Zn^{2+} sites. The linewidths of the EPR signals in Fig. 4 range from 0.011 mT for the axial zinc vacancy to 0.026 mT for the oxygen vacancy. These very small linewidths for the zinc vacancies indicate that the neutron irradiation did not introduce significant random strain in the lattice. The concentration of photoinduced singly ionized oxygen vacancies contributing to the EPR spectrum in Fig. 4 is approximately $2 \times 10^{15} \text{cm}^{-3}$. The concentration of photoinduced singly ionized axial zinc vacancies in Fig. 4 is also approximately $2 \times 10^{15} \text{cm}^{-3}$. These zinc and oxygen vacancies produced by the fast neutrons were destroyed when the crystal was held at 430°C for 10 min.

VI. DISCUSSION

Our results in Figs. 2 and 3(b) show that transmutation of ^{64}Zn to ^{65}Cu has occurred in a ZnO crystal irradiated with neutrons. The observation of the 1115.5 and 511 keV γ rays provides direct evidence that ^{65}Zn nuclei have been formed and are decaying to ^{65}Cu . Furthermore, EPR spectra from the neutron irradiated crystal show that the newly formed ^{65}Cu nuclei are present as Cu^{2+} ions. It is significant that these Cu^{2+} ions were present without laser light. The Cu^{2+} ions in Fig. 3(b) were formed when the ^{64}Zn nucleus of a Zn^{2+} ($3d^{10}$) ion absorbed a neutron and became ^{65}Zn and then decayed to ^{65}Cu by electron capture. This electron-capture process removed one electron from the ion and left a $3d^9$ electron configuration. In other words, a portion of the Zn^{2+} ($3d^{10}$) ions in the regular as-grown lattice directly become paramagnetic Cu^{2+} ($3d^9$) ions (i.e., neutral acceptors) at the zinc sites as a result of the neutron irradiation. The Fermi level in our vapor-transport-grown ZnO crystal

has been lowered by the neutron irradiation and this allows the transmuted Cu^{2+} ions to remain in the A^0 state, as seen in Fig. 3(b). If the Fermi level were higher, these Cu^{2+} ions would convert to Cu^+ ions because of the greater availability of electrons (i.e., an A^0 acceptor would become an A^- acceptor) and laser light would be needed to convert the Cu^+ ions to Cu^{2+} ions.

To further establish the behavior of copper in neutron-irradiated ZnO, the sample used in Fig. 3(b) was heated to 430°C in air for 10 min. The zinc and oxygen vacancies were destroyed (as previously noted), but an EPR spectrum taken at 6 K showed that this heating did not change the copper (i.e., the transmuted Cu^{2+} ions were still seen without light and only hyperfine lines from ^{65}Cu nuclei were present). After this 430°C anneal, the copper ions that were introduced into the sample during growth are still in the form of $\text{Cu}^+\text{-H}$ complexes and do not contribute to the Cu^{2+} EPR spectrum. A final anneal of the neutron-irradiated sample to 900°C for 1 h led to the EPR spectrum in Fig. 5. This spectrum, containing both ^{63}Cu and ^{65}Cu hyperfine lines, was taken at 6 K with the magnetic field in the basal plane. The 900°C anneal dissociated the $\text{Cu}^+\text{-H}$ complexes in the neutron-irradiated sample. Laser light was then needed to convert the isolated Cu^+ ions to Cu^{2+} ions in Fig. 5. This annealed crystal now exhibited the same photoinduced behavior for Cu^{2+} as the non-neutron-irradiated sample in Fig. 3(a). As expected, a comparison of the spectra in Figs. 3(a) and 5 shows that the ratio of the two copper isotopes in Fig. 5 does not agree with the natural abundance ratio of these isotopes. Approximately equal concentrations of ^{63}Cu and ^{65}Cu nuclei are contributing to the hyperfine pattern in Fig. 5 because the transmuted ^{65}Cu nuclei are adding to the ^{63}Cu and ^{65}Cu nuclei that were initially introduced during growth.

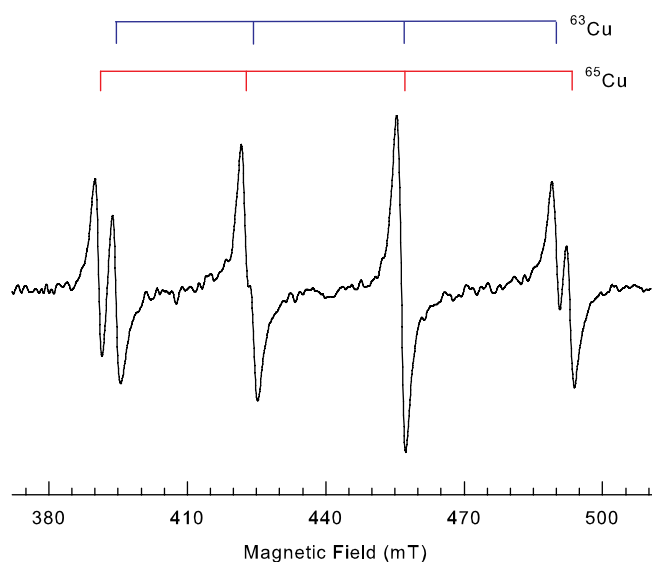


FIG. 5. EPR spectrum of Cu^{2+} ions in the neutron-irradiated ZnO crystal after it was thermally annealed at 900°C in air for 1 h. These data were obtained at 6 K with the magnetic field perpendicular to the c axis and with 442 nm light on the sample. Comparisons should be made with the Cu^{2+} spectra in Fig. 3.

VII. SUMMARY

Nuclear transmutation of ^{64}Zn to ^{65}Cu has been demonstrated in ZnO. A gamma spectrum acquired 10 days after a 20 h irradiation with neutrons shows peaks at 1115.5 and 511 keV, thus verifying that ^{65}Zn has been produced and is decaying to ^{65}Cu . A Cu^{2+} ($3d^9$) EPR spectrum taken 180 days after the neutron irradiation confirms the production of ^{65}Cu by showing that the only hyperfine lines present are from ^{65}Cu nuclei (lines from ^{63}Cu are not seen). The concentration of transmuted ^{65}Cu nuclei in this EPR spectrum is approximately $3.7 \times 10^{16} \text{ cm}^{-3}$. Residual copper impurities inadvertently introduced during growth of the ZnO are observed and fully accounted for in the EPR characterization experiments. EPR was also used to monitor the singly ionized charge states of the zinc and oxygen vacancies produced by the high-energy neutrons. Heating the irradiated crystal to 430°C destroyed these vacancies. In conclusion, our results show that transmutation is a viable process to uniformly dope ZnO with Cu.

ACKNOWLEDGMENTS

The authors thank Adam Brant for help in preparing samples for neutron irradiation and Kevin Herminghuysen at the Ohio State Nuclear Reactor Laboratory for irradiating the samples and recording the gamma spectra. Support for this work at the Air Force Institute of Technology was provided by the Defense Threat Reduction Agency. The views expressed in this paper are those of the authors and do not necessarily reflect the official policy or position of the Air Force, the Department of Defense, or the United States Government.

- ¹R. E. Dietz, H. Kamimura, M. D. Sturge, and A. Yariv, *Phys. Rev.* **132**, 1559 (1963).
- ²R. Dingle, *Phys. Rev. Lett.* **23**, 579 (1969).
- ³A. Hausmann and P. Schreiber, *Solid State Commun.* **7**, 631 (1969).
- ⁴I. Broser and M. Schulz, *Solid State Commun.* **7**, 651 (1969).
- ⁵E. Mollwo, G. Müller, and D. Zwingel, *Solid State Commun.* **15**, 1475 (1974).
- ⁶G. Müller, *Phys. Status Solidi B* **76**, 525 (1976).
- ⁷F. G. Gärtner and E. Mollwo, *Phys. Status Solidi B* **89**, 381 (1978).
- ⁸N. Y. Garces, L. Wang, L. Bai, N. C. Giles, L. E. Halliburton, and G. Cantwell, *Appl. Phys. Lett.* **81**, 622 (2002).
- ⁹E. V. Lavrov, J. Weber, and F. Börrnert, *Phys. Rev. B* **77**, 155209 (2008).
- ¹⁰M. A. Reshchikov, V. Avrutin, N. Izyumskaya, R. Shimada, H. Morkoç, and S. W. Novak, *J. Vac. Sci. Technol. B* **27**, 1749 (2009).
- ¹¹D. Byrne, F. Herklotz, M. O. Henry, and E. McGlynn, *J. Phys.: Condens. Matter* **24**, 215802 (2012).

- ¹²G. K. Lindeberg, *J. Appl. Phys.* **38**, 3651 (1967).
- ¹³H. Kim, K. Park, B. Min, J. S. Lee, K. Cho, S. Kim, H. S. Han, S. K. Hong, and T. Yao, *Nucl. Instrum. Methods Phys. Res., Sect. B* **217**, 429 (2004).
- ¹⁴E. Flitsiyani, C. Swartz, R. E. Peale, O. Lupan, L. Chernyak, L. Chow, W. G. Vernetson, and Z. Dashevsky, *Mater. Res. Soc. Symp. Proc.* **1108**, A05-03 (2009).
- ¹⁵F. A. Selim, M. C. Tarun, D. E. Wall, L. A. Boatner, and M. D. McCluskey, *Appl. Phys. Lett.* **99**, 202109 (2011).
- ¹⁶F. A. Selim, M. C. Tarun, D. E. Wall, L. A. Boatner, and M. D. McCluskey, *Appl. Phys. Lett.* **101**, 029901 (2012).
- ¹⁷M. C. Recker, "Copper doping of zinc oxide by nuclear transmutation," M.S. Thesis, Air Force Institute of Technology, Wright-Patterson AFB, Dayton, OH, 2014.
- ¹⁸Y. Kanai, *Jpn. J. Appl. Phys., Part 1* **30**, 703 (1991).
- ¹⁹E. Mollwo, G. Müller, and P. Wagner, *Solid State Commun.* **13**, 1283 (1973).
- ²⁰G. Müller and R. Helbig, *J. Phys. Chem. Solids* **32**, 1971 (1971).
- ²¹S. Lautenschlaeger, M. Hofmann, S. Eisermann, G. Haas, M. Pinnisch, A. Laufer, and B. K. Meyer, *Phys. Status Solidi B* **248**, 1217 (2011).
- ²²O. Volnianska, P. Boguslawski, and E. Kaminska, *Phys. Rev. B* **85**, 165212 (2012).
- ²³D. B. Buchholz, R. P. H. Chang, J. H. Song, and J. B. Ketterson, *Appl. Phys. Lett.* **87**, 082504 (2005).
- ²⁴D. Chakraborti, J. Narayan, and J. T. Prater, *Appl. Phys. Lett.* **90**, 062504 (2007).
- ²⁵Z. A. Khan and S. Ghosh, *Appl. Phys. Lett.* **99**, 042504 (2011).
- ²⁶S. Y. Zhuo, X. C. Liu, Z. Xiong, J. H. Yang, and E. W. Shi, *AIP Adv.* **2**, 012184 (2012).
- ²⁷J. R. De Laeter, J. K. Böhlke, P. De Bièvre, H. Hidaka, H. S. Peiser, K. J. R. Rosman, and P. D. P. Taylor, *Pure Appl. Chem.* **75**, 683 (2003).
- ²⁸See <http://www.nndc.bnl.gov/sigma/> for Evaluated Nuclear Data File, National Nuclear Data Center, Brookhaven National Laboratory (2011).
- ²⁹M.-M. Bé, *Appl. Radiat. Isot.* **64**, 1396 (2006).
- ³⁰K. Kossert, H. Janssen, R. Klein, M. Schneider, and H. Schrader, *Appl. Radiat. Isot.* **64**, 1420 (2006).
- ³¹U. Schötzg, *Nucl. Instrum. Methods Phys. Res. A* **286**, 523 (1990).
- ³²See <http://www.nndc.bnl.gov/chart/> for Chart of Nuclides, National Nuclear Data Center, Brookhaven National Laboratory (2014).
- ³³N. Y. Garces, N. C. Giles, L. E. Halliburton, G. Cantwell, D. B. Eason, D. C. Reynolds, and D. C. Look, *Appl. Phys. Lett.* **80**, 1334 (2002).
- ³⁴R. B. Firestone, *Table of Isotopes*, 8th ed., edited by C. M. Baglin and S. Y. F. Chu (John Wiley and Sons, Hoboken, NJ, 1999).
- ³⁵The solid angle for detection (in our gamma spectrometer) is approximately 2π steradians, thus one-half of the emitted 1115.5 keV γ rays enter the detector while one γ ray from each pair of 511 keV γ rays (emitted in opposite directions) enters the detector.
- ³⁶F. Börrnert, E. V. Lavrov, and J. Weber, *Phys. Rev. B* **75**, 205202 (2007).
- ³⁷J. Hu and B. C. Pan, *J. Phys. Chem. C* **112**, 19142 (2008).
- ³⁸N. Y. Garces, L. Wang, N. C. Giles, L. E. Halliburton, G. Cantwell, and D. B. Eason, *J. Appl. Phys.* **94**, 519 (2003).
- ³⁹S. J. Jokela and M. D. McCluskey, *J. Appl. Phys.* **107**, 113536 (2010).
- ⁴⁰N. J. Stone, *At. Data Nucl. Data Tables* **90**, 75 (2005).
- ⁴¹J. M. Smith and W. E. Vehse, *Phys. Lett.* **31A**, 147 (1970).
- ⁴²A. L. Taylor, G. Filipovich, and G. K. Lindeberg, *Solid State Commun.* **8**, 1359 (1970).
- ⁴³D. Galland and A. Hervé, *Phys. Lett.* **33A**, 1 (1970).
- ⁴⁴K. Leutwein and J. Schneider, *Z. Naturforsch., A: Phys. Sci.* **26**, 1236 (1971).